A genome-scale metabolic model of *Saccharomyces cerevisiae* that integrates expression constraints and reaction thermodynamics

Omid Oftadeh[1], Pierre Salvy[1], Maria Masid[1], Maxime Curvat[1], Ljubisa Miskovic[1], Vassily Hatzimanikatis[1*]

[1]Laboratory of Computational Systems Biotechnology, École Polytechnique Fédérale de Lausanne (EPFL), CH 1015 Lausanne, Switzerland

*Corresponding author. E-mail: vassily.hatzimanikatis@epfl.ch

Keywords: Metabolic and expression model, *Saccharomyces cerevisiae*, Genome-scale metabolic models, Mixed-integer linear programming, Expression system

Abstract

Eukaryotic organisms play an important role in industrial biotechnology, from the production of fuels and commodity chemicals to therapeutic proteins. To optimize these industrial systems, a mathematical approach can be used to integrate the description of multiple biological networks into a single model for cell analysis and engineering. One of the current most accurate models of biological systems include metabolism and expression (ME-models), and Expression and Thermodynamics FLux (ETFL) is one such formulation that efficiently integrates RNA and protein synthesis with traditional genome-scale metabolic models. However, ETFL is so far only applicable for *E. coli*. To therefore adapt this ME-model for *Saccharomyces cerevisiae*, we herein developed yETFL. To do this, we augmented the original formulation with additional considerations for biomass composition, the compartmentalized cellular expression system, and the energetic costs of biological processes. We demonstrated the predictive ability of yETFL to capture maximum growth rate, essential genes, and the phenotype of overflow metabolism. We envision that the extended ETFL formulation can be applied to ME-model development for a wide range of eukaryotic organisms. The utility of these ME-models can be extended into academic and industrial research.

Introduction

Eukaryotic organisms are extremely important in industrial biotechnology (e.g., *Saccharomyces cerevisiae*[1] and *Yarrowia lypolytica*[2]) and are host organisms for the production of fuels and specialty and commodity chemicals. Also eukaryotic, mammalian systems such as Chinese hamster ovary (CHO) cells are the main platform organism used for therapeutic protein production[3]. In contrast to bacterial cells, the eukaryotes have compartmentalized cell structure to localize macromolecules with different biological tasks. This fundamental difference renders the engineering of the eukaryotes more complex and challenging. To help optimize and plan for industrial applications, complex biological systems such as these can be represented *in silico* by specific networks designed to capture key processes.

Metabolic networks are the most widely studied and modeled type of biological networks, with over 6,000 genome-scale metabolic models (GEMs) reconstructed for archaea, bacteria, and eukaryotes[4, 5]. One approach for analyzing these models is Flux Balance Analysis (FBA), which is a constraint-based optimization technique, where the metabolic flux of individual reactions are computed in a metabolic network by formulating a linear optimization problem[6]. However, FBA can predict biologically irrelevant solutions, including cycles with unrealistically high fluxes[7] or thermodynamically infeasible solutions[8, 9]. Despite its wide applicability, FBA cannot predict some important features of metabolic networks, such as those that account for limited catalytic capacity of enzymes or limitations in cellular expression systems.

To overcome some of the issues with FBA and eliminate unrealistic solutions, additional constraints that represent empirical or mechanistic evidence have been introduced. For example, Thermodynamic-Based Flux Balance Analysis (TFA)[8, 9] enforces the coupling between the directionality of each reaction with its corresponding Gibbs free energy to eliminate thermodynamically infeasible predictions. More importantly, TFA also directly integrates variables for the concentrations of metabolites, which enables the integration of metabolomics data. Genome-Scale Models with Enzymatic Constraints using Kinetic and Omics data (GECKO) is another FBA-based method that accounts for the limited catalytic activity of enzymes by inclusion of enzyme concentrations as variables[10]. Previous studies have shown that GECKO can capture a realistic maximum specific growth rate and the occurrence of overflow metabolism in *Saccharomyces cerevisiae*[10]. However, GECKO does not

explicitly consider the cost of protein synthesis. Instead, it assumes that the fractions of peptides within a protein pool are inversely proportional to their molecular weight. The molecular weight represents the cost of the enzyme within the context of proteome allocation. However, the actual cost of enzyme synthesis is absent from the formulation. Therefore, GECKO fails to account for the competition for amino acids required for enzyme synthesis, which is an important part of the expression system.

Metabolic and Expression models (ME-models) are another class of constraint-based models that include the cellular expression system in addition to metabolic and catalytic constraints[11-13]. ME-models include individual mRNA and enzyme concentrations as well as their cost of synthesis and cellular expression capacity. A new approach to construct ME-models, called expression and thermodynamics-enabled flux (ETFL)[13], was recently proposed to address the significant drawback of needing to solve the nonlinear programming (NLP) problem. The approach avoids bilinear terms by discretizing growth and solving locally linearized mixed-integer problems instead of a NLP problem. Similar to published ME-models[11, 14], the first ETFL model was developed for *Escherichia coli*. However, the ETFL formulation can readily be extended to the study of eukaryotic organisms.

S. cerevisiae is an industrially relevant organism[1, 15] that is widely used for biological and medical research studies[16]. Several GEMs of this organism have been published over the years due to its ubiquity in metabolic engineering[17-22]. However, likely due to additional requisite considerations in modeling the compartmentalized cellular expression systems of eukaryotes, no ME-model of *S. cerevisiae* has been developed. The previous ME-models were constructed for bacteria[11-13], with one ribosome and one RNA polymerase being sufficient to represent the cellular expression machinery. In contrast, *S. cerevisiae* as a eukaryotic organism additionally has mitochondrial ribosomes and RNA polymerases. In this work, we extended the ETFL formulation and code for applicability to eukaryotic systems. In this new formulation, we account for the additional ribosomes and RNA polymerases within the eukaryotic mitochondrial expression system. We also included an allocation constraint for the fraction of proteins that are allocated to metabolism and cellular expression. Herein, we propose an ETFL model for *S. cerevisiae*, named yETFL, which is based on the extended ETFL formulation. The methodological advancements in ETFL provide avenues towards development of such models for the study of other eukaryotes.

Results and Discussion

Model Description

In this work, we present an ETFL model for *S. cerevisiae*, named yETFL (Table 1). yETFL is based on the latest *S. cerevisiae* genome-scale model Yeast8. Towards the generation of yETFL, we first performed a thermodynamic curation of Yeast8, which contains 1326 unique metabolites (a total of 2691 compartmentalized metabolites), 3991 reactions, 1149 genes, and 14 compartments (including the extracellular space). There are 2614 reactions that are associated to genes.

Information about the thermodynamic properties of reactions allows us to (i) integrate the available metabolomics and fluxomics data into the models, (ii) compute thermodynamically consistent values of metabolic fluxes and metabolite concentrations, and (iii) determine thermodynamically feasible directionalities. Using the group contribution method (GCM), we estimated the Gibbs free energies of formation for 1092 of 1326 total unique metabolites. We then estimated the Gibbs free energies for 1880 reactions in the Yeast8 GEM, which only includes reactions in an aqueous environment (see Materials and Methods). Yeast8 has 1304 reactions in the membrane compartments (non-aqueous environment). We did not apply thermodynamic constraints for these 1304 reactions as thermodynamic relations for membrane-associated metabolites require correction based on information about the non-aqueous environments, which is not always available.

In yETFL, we modeled the synthesis of 1059 enzymes coupled to 2588 of 2614 reactions with associated genes. The catalytic constraints are specified by coupling the reactions and the enzymes, which requires information on k_{cat}, or the enzyme turnover numbers. We found k_{cat} values for 943 enzymes and approximated this number for a further 166 enzymes from the median k_{cat} value in *S. cerevisiae* (see Materials and Methods). Of these enzymes, 77 were transporters associated to 167 transport reactions, there are 107 complexes among the enzymes, and the remainder are monomeric enzymes composed of a single peptide. A complexation reaction is considered for each enzyme to account for its synthesis from the constituent peptides.

While one RNA polymerase and one ribosome can sufficiently represent bacterial expression system, in a eukaryotic cell such as *S. cerevisiae*, there are different RNA polymerases and ribosomes. Notably, the mitochondria have their own RNA polymerase and ribosome. The extended ETFL formulation, presented here, enables

implementing multiple ribosomes and RNA polymerases, the latter of which includes: (i) the RNA polymerase II, which transcribes nuclear genes and (ii) the mitochondrial RNA polymerase, which transcribes the mitochondrial genes. The model also includes three ribosomes, where one ribosome is associated with mitochondrial genes and the other two ribosomes are associated with nuclear genes, but differ in their composition (see Materials and Methods). Altogether, yETFL includes 1149 metabolic genes from Yeast8 and an additional 244 genes that encode the composition of the aforementioned ribosomes and RNA polymerases.

To study the inclusion or exclusion of thermodynamic constraints and a variable or constant type of resource allocation (Materials and Methods), we developed four different types of models (Table 2). The inclusion of thermodynamic constraints is reflected by the presence of "T" in the name of the model (i.e., ETFL.cb and ETFL.vb), and the "cb" points to a version with a constant biomass composition, while "vb" indicates the biomass composition is variable with growth. The number of variables and constraints in each model is detailed in Table 2. We used 128 bins to discretize the growth in the range of [0, μ_{max}], where μ_{max} is the maximum growth rate of *S. cerevisiae* as observed in rich growth medium (see Salvy and Hatzimanikatis[13] for details). This resulted in 135 (i.e., $128 + \log_2 128$) binary variables in the models without thermodynamic constraints, denoted as EFL.cb and EFL.vb. In the models with thermodynamic constraints, two binary variables were added per reaction to account for the directionality, which resulted in 8073 binary variables.

Prediction of specific growth rate

The cellular growth rate should plateau when high values of substrate uptake are attained, as limitations in the expression system and catalytic activity of enzymes cause shift the growth rate from a glucose-dependent limitation to an enzyme-dependent one. This phenomenon is described by established empirical models of microbial growth, where the growth shifts from nutrient limitation to proteome limitation[23]. However, standard FBA models predict that the growth rate increases linearly with increased carbon uptake. Since ETFL accounts for expression limitations, it is expected to predict this shift in the cellular growth rate.

We investigated the variations in growth rate with constant (E[T]FL.cb) and variable (E[T]FL.vb) biomass composition by examining the predicted maximum growth rate versus the glucose uptake (Figure 1). With a constant biomass composition,

the stoichiometric coefficients are constant in the growth reaction. Likewise, the stoichiometric coefficients change with growth in the variable composition. In both cases, and in contrast to FBA, the growth rate plateaued at higher values of glucose uptake rate, which is in accordance with the experimental results[24]. That is, we observed a shift from glucose-limited growth to proteome-limited growth. The maximum predicted growth rate was 0.46 h^{-1} and 0.42 h^{-1} for E(T)FL.cb and E(T)FL.vb, respectively. Both agree with experimentally measured maximum growth rates reported in the literature, which are in the range of 0.4–0.45 h^{-1} for different strains[25-27]. The accuracy of our predictions with experimental observations is important, as the maximum growth rate was highly overestimated in previously reported ME-models[12, 13], likely due to the lack of an allocation constraint on the total amount of metabolic enzymes (see Eq. 5). Integration of this allocation constraint into the yETFL formulation was straightforward, but previous ME-model formulations disallowed the addition of this constraint without fundamental modification of the solving process[14].

We observed small discrepancies in the maximal growth rate between the experimental data and the yETFL results for the glucose uptake rate, which ranged from ~4 mmol/gDW/h to ~11 mmol/gDW/h (Figure 1). One cause of these discrepancies might be the growth dependence of certain parameters, such as the ribosomal elongation rate. To avoid excessive constraints in the model and to preserve experimental observations with a feasible solution space, we used the highest reported values for ribosomal elongation rate, which typically corresponds to higher growth rates[28, 29]. Since our formulation accounts for growth-dependent parameters, we anticipate the facile integration of new information on the variation of the parameters with the growth rate into yETFL.

Another contributor to experimental and predicted discrepancies might be the regulation system that is used by *S. cerevisiae* during the transition from nutrient-limited to proteome-limited growth. Like other ME-models, yETFL works under the assumptions of optimality (e.g., maximal growth rate) and that the cellular system evolved under selection pressure to match this optimality. In this context, the regulatory network of *S. cerevisiae* can be seen as a control system that drives the metabolism towards optimality. Deviations from model optimality in transition regions are simply limitations of the regulatory system. Therefore, the predictive ability of the model can be enhanced by the addition of regulatory constraints from improved input on mechanisms and parameters that regulate the phenotypic transition.

Gene Essentiality Analysis

To investigate the quality of yETFL, we examined the ability of the model to predict which genes are essential for the cellular growth. We discovered that the gene essentiality results for metabolic genes were identical for the EFL.cb and FBA models (Table 3A). This includes 1149 genes associated with metabolic reactions in the Yeast8 model. We compared the predicted essentialities to the experimental observations, which were available for 5061 genes, to assess the quality of the model. However, this is not comprehensive of *S. cerevisiae* genes. The results in Table 3A show the essentiality of metabolic genes with the available experimental data. Compared to the FBA model, yETFL models have more genes that correspond to RNA polymerases and ribosomes (expression genes). We could not do gene essentiality for these 244 expression genes with FBA, as these genes are not associated to any function in the Yeast8 model. There are 222 expression genes with available experimental data that are represented alongside the metabolic genes in Table 3B. From these results, we performed gene essentiality for a greater number of genes in yETFL (1393 genes) than in Yeast8 (1149 genes), with a slight improvement in the Matthews correlation coefficient (Table 3). We also found that the integration of thermodynamic constraints into FBA or EFL.cb did not change the essentiality results.

Crabtree Effect

Overflow metabolism is a shift from an optimal to a non-optimal metabolic phenotype and is observed in different organisms at high growth rates[24, 30, 31]. Overflow metabolism in *S. cerevisiae*, also called the Crabtree effect, occurs when cells shift from pure respiration to a combination of respiration and fermentation in the presence of oxygen. This happens after cells reach a critical growth rate, which is strain-specific though can be estimated at about 0.3 h^{-1}. Because one hypothesis for why overflow metabolism occurs is proteome limitation[32, 33] and because the yETFL model takes this into account, we therefore next looked at the ability of yETFL to predict this metabolic shift.

The Crabtree effect in *S. cerevisiae* cannot be predicted with FBA unless some *ad hoc* assumptions are made in the constraints or the objective function[33]. In contrast, we successfully predicted the shifts in fluxes at higher growth rates with yETFL, which considered limitations in the catalytic capacity of the enzymes and protein expression machinery (Figure 2). In fact, yETFL could capture the shift in metabolism at high

growth rates, where ethanol was secreted, and CO_2 production increased while O_2 consumption decreased. The model had good qualitative agreement with the experimental data acquired from aerobic, glucose-limited chemostat cultures[24].

The E[T]FL.vb models (see Materials and Methods) presented an earlier onset of the Crabtree effect relative to the E[T]FL.cb models (Figure 2). We can attribute the onset to the Yeast8 protein fraction used in E[T]FL.cb, which is close to the experimentally observed values at higher growth rates. Thus, the E[T]FL.cb models are less constrained than the E[T]FL.vb ones. In general, models with higher protein ratios are less tightly constrained. Hence, their maximum growth rate and the Crabtree effect occur at higher growth rates (Figure 2). We also observed a slight deviation of the model predictions from the experimental observations in the transition region for the growth rates between 0.3 and 0.38 h^{-1}, the onset of Crabtree effect with the experimental data and yETFL, respectively (Figure 2). A potential method to enhance the predictive ability of yETFL in light of these slight discrepancies would be through the inclusion of regulatory mechanisms by integration of regulatory constraints. Another next step would be to account for the growth dependence of more parameters. These improvements can be facilitated by further experimental investigations into *S. cerevisiae* physiology.

It is of note that yETFL was able to capture the Crabtree effect solely by integration of experimentally measured data and without *ad hoc* modifications in the model or the formulation. In an earlier study[10], an additional parameter was introduced to further constrain the availability of enzymes. Since the saturation rate of individual enzymes is not known, this parameter was introduced as the saturation rate of the total enzymatic pool and it was calculated by fitting the model predictions to the experimental data. Here, we captured the Crabtree effect without additional parameters, as yETFL explicitly accounts for the saturation rates of individual enzymes. Moreover, yETFL also allows for integration of experimentally observed saturation rates of individual enzymes by the addition of saturation parameters to the catalytic constraint of each enzyme. These parameters can then be found by fitting the model predictions to the experimental data, as has been reported[34]. Following a similar procedure, we can also integrate different experimental transcriptional and translational efficiencies into the model.

Conclusion

In this work, we developed a model for a eukaryotic organism, *S. cerevisiae,* by extension of the recently published formulation of ETFL to consider compartmentalized expression systems with separate ribosomes and RNA polymerases. This is the first model for yeast that includes RNA and enzyme concentration data, and this explicit simulation of expression broadens the applications of yETFL to the simulation of the impacts of different perturbations on cellular mechanisms. To test the accuracy of yETFL, we validated the predictions of the model against experimental data. Moreover, we reproduced the emergence of the Crabtree effect, and observed the secretion of ethanol in aerobic conditions without needing to integrate experimental data as with previous descriptions of the Crabtree effect[10].

Overall, a key advantage of the ETFL formulation is its direct extension to other types of analyses, such as the study of the Crabtree effect at the steady-state as we have presented in this work. Future work in understanding the emergence of this effect in a dynamic setting, as previously shown for the *E. coli* overflow metabolism[35], will yield valuable insights on the optimality of the regulatory mechanisms in *S. cerevisiae*. We envision that this information can be applied to design industrially valuable strains. Also, yETFL can be used as a scaffold to integrate other biological networks, such as regulatory or signaling networks[5], as a vital step towards constructing a whole-cell model[36]. Finally, the extension of the ETFL formulation presented here is readily adaptable to any eukaryotic organism for which a well-curated GEM is available. The quality of the information about enzymes (i.e., catalytic rate constants and protein composition) will affect the quantitative predictions of the model, though new data is easily inputted into ETFL such that the predictions will always be as good as the available data. We envision that the availability of eukaryotic ME-models will improve the understanding and engineering of industrial hosts for the refinement and creation of better eukaryotic systems in biotechnology, for applications ranging from the production of fuels and commodity chemicals to therapeutic proteins.

Materials and Methods

Formulation of the ETFL model

yETFL is based on the ETFL formulation, which was previously described in detail in Salvy and Hatzimanikatis.[13]. The ETFL constraints can be divided into five main categories:

- **Metabolic constraints:** Enforce all metabolite and macromolecule concentrations to be at steady-state. These constraints are the same as in FBA[6].
- **Thermodynamic constraints:** Couple the directionality of reactions with their Gibbs free energy. These constraints are the same as in TFA[8, 9].
- **Catalytic constraints:** Define upper bounds on the reaction fluxes based on the enzymatic capacity of the associated enzymes.
- **Expression constraints:** Model the synthesis of mRNAs, peptides, and proteins, and constrain synthesis rates based on the limitations of transcription and translation machinery.
- **Allocation constraints:** Determine the available amounts of DNA, RNA, and proteins in the cell. If experimental data is available, the ETFL formulation allows for modeling the growth-dependent abundance of these macromolecules. Whenever the experimentally measured abundance of these macromolecules during growth is not available, we assume that the ratio between these quantities is growth-independent, an assumption already made in FBA.

Data Collection

Genome-scale Metabolic Model

The most recent GEM of *Saccharomyces cerevisiae,* Yeast8[22], was used as a basis to construct the yETFL model. The latest published version of Yeast8 model, Yeast8.3.4, was obtained from the GitHub as it was provided by Laboratory of Systems and Synthetic Biology at Chalmers University (https://github.com/SysBioChalmers/yeast-GEM).

The following modifications to Yeast8 were made:

- Pseudometabolites defined for RNAs and proteins as well as pseudoreactions defined for their synthesis were replaced by the explicit expressions for RNAs

and protein synthesis **(**according to the procedure described in Salvy and Hatzimanikatis[13]**)**.

- tRNAs and their reactions were adapted into a formulation that accounts for dilution effects, according to the ETFL procedure[13]**.** This is necessary as the dilution effect is not necessarily negligible for tRNAs.
- The biomass reaction was modified to account for growth-dependent composition, as discussed in detail in the section Allocation Data and Constraints**.**

Thermodynamic curation of Yeast8

We used Group Contribution Method (GCM)[37] to determine the standard Gibbs free energy of formation in aqueous, ionic environments[38] for 1092 out of 1326 (82.4%) unique metabolites from Yeast8 (Figure 3). We were not able to determine the thermodynamic properties for the remaining 234 metabolites because: (i) 89 metabolites (6.7%) represented abstract compounds, such as pools of proteins, nucleotides, lipid chains; (ii) 92 metabolites (6.9%) did not have a known molecular structure or they contained structural groups for which the estimated standard Gibbs energy of formation is unknown (e.g., acyl carrier protein group); and (iii) 53 metabolites (4%) contain groups with unknown energy in their composition. Using the standard Gibbs free energy of formation of compounds, we integrated the thermodynamic properties only for reactions in the aqueous solution. We estimated the standard Gibbs free energy of reactions for 1880 out of 2687 (70.0 %) such reactions from Yeast8. The standard Gibbs free energy of reactions with at least one metabolite associated with a membranous compartment (including 1304 reactions) was not calculated using this procedure, as the standard Gibbs free energy of formation of compounds was determined for the aqueous environments.

mRNA, Peptide, and Protein Data

The sequences for the peptides and mRNAs were obtained from the KEGG database[39]. Information about the stoichiometry of peptides forming enzymatic complexes in *S. cerevisiae* was obtained by combining available information in YeastCyc[40] and Complex Portal[41]. Turnover numbers (k_{cat}) were retrieved from BRENDA using functions provided by GECKO[10].

Allocation Data and Constraints

We created yETFL models using either a constant or variable biomass composition. For constant biomass composition (E[T]FL.cb), we used the macromolecular fractions from the Yeast8 biomass reaction. The mass fractions for different macromolecules were calculated using the equation:

$$f_k = \sum_{i \in M_k} \eta_i MW_i \,. \tag{1}$$

For each type of macromolecule, M_k, $\eta_{i \in M_k}$ is the stoichiometric coefficient of the metabolites belonging to this macromolecule class in the biomass reaction, and MW_i is their molecular weight. For example, to find the protein fraction in the biomass, f_{Prot}, the stoichiometric coefficients of individual amino acids were multiplied by their molecular weight to find their mass fractions in the biomass. The sum of these amino acid ratios indicates how much of the biomass is protein. By definition, the weight of biomass should be 1 gram[42, 43], i.e.,

$$\sum_{i \in BBBreactants} \eta_i MW_i - \sum_{j \in byproducts} \eta_j MW_j = 1. \tag{2}$$

In this equation, *BBBreactants* is the set of reactants in biomass reaction and *byproducts* is the set of all products except biomass.

When generating an ETFL model, it is important to remove protein and RNA metabolites from the biomass equation to prevent double-counting of the metabolic requirements, since the explicit mRNA and peptide synthesis reactions already account for their respective participation in cell growth.

In ETFL, we model the participation of macromolecules in the cellular biomass composition as follows:

$$\sum_j MW_j E_j = P^m, \tag{3}$$

$$\sum_l MW_l F_l = R^m \,, \tag{4}$$

where P^m and R^m are, respectively, the protein and RNA mass fractions in *g/gDW*, and E_j and F_l represent, respectively, the concentration of enzyme j and RNA l in *mmol/gDW*. P^m and R^m can either be constant (E[T]FL.cb) or variable and discretized (E[T]FL.vb).

To create an E[T]FL.vb model, it is necessary to know the fraction of each biomass component at different growth rates. We gathered this information for *S. cerevisiae* by reviewing the literature (data available on the online ETFL repository, see Code and Dependencies)[24, 44, 45]. Since the data is usually reported for a few particular growth rates, we resampled it using piecewise-linear interpolation.

Protein allocation

Since ME-models do not consider all the cellular tasks of proteins, ETFL defines a generic, so-called dummy protein to represent the fraction of the proteome not accounted for in the model[13], such as structural proteins, signaling proteins, or chaperones. However, since the dummy protein is not associated with a cellular function, the optimization procedure will apportion the whole protein content to the proteins that are associated with a cellular task (i.e., metabolic enzymes, ribosomal peptides, and RNA polymerase). Consequently, the concentration of the latter proteins is overestimated, which results in overestimating the maximum growth rate, and the Crabtree effect emerges at higher growth rates. To realistically account for enzyme participation in the proteome, we can define φ, the proportion of proteins that is associated with a metabolic task, in the total protein content of the cell. Then, we can add the following constraint in the optimization problem:

$$\sum_{j \neq dummy\ protein} MW_j E_j = \varphi \cdot P^m \,. \tag{5}$$

This way, the constraints in Eq. 3 and 5 enforce the optimization procedure to allocate a fraction of the proteome, i.e., $(1-\varphi)$, to the proteins with cellular functions not considered in the model, i.e., dummy protein. We used the latest protein abundance dataset for *S. cerevisiae* available in PaxDB[46] to compute this fraction as $\varphi = 0.55 g/g_{protein}$.

DNA

The growth dependence of the DNA abundance in the cell was modeled as proposed in the original ETFL formulation[13].

Carbohydrates, Lipids, and Ions

To consider the growth dependence of the biomass composition, we introduced the variation of the other biomass components in the ETFL formulation. To this end, we

first defined a metabolite pool for each of these macromolecules. In Yeast8, each biomass component is attached to a pooling reaction that transforms the sum of specific metabolites (e.g. all carbohydrate metabolites) into a single metabolite pool (e.g. carbohydrate). The mass balance equation for these modeling metabolites is the following:

$$\frac{d[X_i]}{dt} = \eta_i^{biomass}\mu - \eta_i^{pool}v_i^{pool} \in \{Carbohydrate, Lipid, Ion\}, \quad (6)$$

where v_i^{pool} is the flux through the pooling reaction, and η_i^{pool} and $\eta_i^{biomass}$ represent stoichiometric coefficients of the modeling metabolite *i* in the pooling and biomass reactions, respectively. When it is desired to model a growth-dependent stoichiometric coefficient in the biomass reaction, the said stoichiometric coefficient can be redefined as a function of μ and calculated as follows:

$$\eta_i^{biomass} = \eta_{i,\ ref}^{biomass}\frac{X_{u,i}^m}{X_{ref,i}^m}, i \in \{Carbohydrate, Lipid, Ion\}. \quad (7)$$

In this equation, $X_{u,i}^m$ is the discretized mass fraction of component *i* in the discretized growth state number *u*, following notations from Salvy and Hatzimanikatis[13]. $\eta_{i,\ ref}^{growth}$ is the stoichiometric coefficient in the biomass reaction, and $X_{ref,i}^m$ is the mass ratio of component *i* in a reference model (e.g. FBA).

Ribosomes and RNA Polymerases

To model the ribosomes and the RNA polymerases, information about their constituting peptides, ribosomal RNA, and catalytic rate constants is required. To consider the eukaryotic complexity of *S. cerevisiae*, we defined multiple RNA polymerases and ribosomes in yETFL (Table 1):

- **RNA polymerase**: Similar to the other eukaryotes, *S. cerevisiae* has three different types of nuclear RNA polymerases. However, most of the mRNA transcripts are transcribed by RNA polymerase II[47]. In yETFL, we implemented this nuclear RNA polymerase, and we modeled such that all the nuclear genes could be transcribed only by this enzyme, similar to the previous work[13]. For mitochondrial genes, we defined a mitochondrial RNA polymerase, which was characterized by its own composition and kinetic parameters[47].
- **Ribosome**: The structure of the cytosolic ribosomes in *S. cerevisiae* contains four ribosomal RNA (rRNA) molecules encoded by four different genes. In addition to these four rRNAs, the cytosolic ribosomes contain 78 peptides

encoded by 137 genes[48]. Out of 78 peptides, 19 are encoded by a single gene and 59 peptides are encoded by either of two alternative genes. To account for alternative ribosomal peptides, we defined two sets of genes: set A containing 59 genes encoding for the 59 peptides (designated with "A" in their standard names, e.g., RPL1A), and set B containing the alternative genes of set A (designated with "B" in their standard names, e.g., RPL1B). Then, we constructed two cytosolic ribosomes, one where we constructed the 59 peptides using the set A and the other where we used the set B. We assumed a similar elongation rate for both cytosolic ribosomes.

A mitochondrial ribosome was also defined to translate mitochondrial genes. This ribosome is composed of two rRNAs and 78 peptides[49].

Modifying the Growth-associated Maintenance

The energetic cost of growth, including maintenance of the cell and polymerization of the macromolecules[50], is quantified in genome-scale models using the growth-associated maintenance (GAM). In ETFL, we consider the energetic cost of protein synthesis explicitly, and this cost should be removed from the GAM to avoid the overestimation of energetic requirements in the polymerization of peptides (Eq. 8).

$$\begin{aligned}\sum_{aa_i \in A} \eta^l_{aa_i}\, tRNA^{charged}_{aa_i} + 2L^l_{aa}(GTP + H_2O) \\ \rightarrow\ Pep_l \\ + \sum_{aa_i \in A} \eta^l_{aa_i}\, tRNA^{uncharged}_{aa_i} \\ + 2L^l_{aa}(GDP + Pi + H^+),\end{aligned} \tag{8}$$

where aa_i is the i^{th} amino acid, $\eta^l_{aa_i}$ represents its count in the lth peptide (Pep_l), and L^l_{aa} is the length of the peptide in amino acid.

Since 2 moles of GTP are needed to attach 1 mole of amino acid to the peptide (Eq. 8), and from

$$ATP + GDP \rightarrow ADP + GTP, \tag{9}$$

1 mole of ATP is required to produce 1 mole of GTP. Therefore, we can deduce that peptide polymerization requires 2 moles of ATP per 1 mole of amino acid.

We also know that the stoichiometric coefficients of amino acids in the biomass reaction of Yeast8 give information on how many *mmol/gDW* of each amino acid are required to produce 1 gram of biomass. From there, it is straightforward to compute the total amount of amino acids (~4.1 *mmol*) required for the production of 1 gram of biomass. Combined, we can calculate that to produce 1 gram of biomass, the energetic cost is $2 \times 4.1 = 8.2$ *mmol/g*DW of ATP for peptide synthesis, which we removed from the GAM.

Gene-protein-reaction Coupling

Coupling the reactions in metabolic networks with their enzymes is the most important step in the process of creating an ETFL model. Ideally, assigning enzymes to reactions requires information about: (i) gene-protein-reaction rules; (ii) catalytic rate constants (k_{cat}); and (iii) type and stoichiometry of the peptide assembly into enzymes. Whenever we did not have access to all required information, we made the following assumptions (Figure 4):

- We assumed similar composition for isoenzymes if composition information was only available for one of them. For example, if one of the isoenzymes is a dimer, the other is also assumed to be a dimer.
- We assumed that monomeric enzymes catalyze reactions (i) that depend on a single gene, and (ii) for which information about their enzyme composition was not available.
- If an enzyme peptide composition is identified, either from databases or by approximation, but its k_{cat} was not found, we set the k_{cat} equal to 70.9 s^{-1}, which is the median for k_{cat}s in *S. cerevisiae*[10].
- While the reactions that transport a metabolite from one compartment to another one are associated with genes, their k_{cat} information is scarce. As a result, these reactions were not catalytically constrained in similar models such as GECKO[10]. We set k_{cat} of the proteins that catalyze these reactions to a large number (1E+9 h^{-1}), which ensures that these reactions are not catalytically constrained and only the gene-protein-reaction relationship is preserved. We also checked the impact of constraining the transport reactions. To this end, these reactions were constrained by the median k_{cat}, but no significant change was observed in the results.

Gene Essentiality Analysis

We used gene essentiality analysis[51] to assess the quality of yETFL. The ETFL formulation enables single-gene knockouts by blocking the flux through transcription reaction for each gene. The predicted essential genes were compared against experimental data for *S. cerevisiae* obtained from http://www-sequence.stanford.edu/group/yeast_deletion_project/downloads.html. Before deleting the genes, the culture medium was modified according to Lu *et al.*[22]. Briefly, the minimal medium supplemented with amino acids and nucleotides was used for the simulations, and the model was allowed to uptake glucose as the sole carbon source. The Matthew's correlation coefficient (MCC) was used as a metric to evaluate the quality of predictions for FBA and ETFL because of its robustness to the imbalance in the number of essential and non-essential genes. MCC can take values from -1 to 1, where values of MCC close to -1 indicate predictions opposed to the ground truth, 0 random predictions, and 1 perfect predictions.

Chemostat Simulations

The results of this paper were obtained by simulating the cell growth as a function of different carbon uptake rates. This allows the exhibition of proteome-limited behavior and overflow metabolism in the presence of excess glucose. For all simulations, the model was allowed to uptake glucose as a carbon source, some essential inorganic compounds, and oxygen. To prepare the model for the simulations, it was modified as described previously in Sánchez *et al.*[10].

To capture the Crabtree effect, the substrate uptake rate was minimized for different values of the growth rate. Then, we fixed the values of the substrate uptake rates at the computed minima and minimized the total fluxes[52] and then the total enzyme concentrations[10], consecutively, to account for the parsimonious enzyme usage. Finally, the Chebyshev center of the enzyme space was used as a representative solution[35].

Code and Dependencies

The code was implemented in Python 3.7, and the commercial solver Gurobi was used to solve the MILP problems. The code relies on the ETFL[13] and pyTFA[53] packages, which use COBRApy[54] and Optlang[55]. The code to generate yETFL models and reproduce the results of this paper is freely available at https://github.com/EPFL-

LCSB/etfl/tree/dev_yetfl and https://gitlab.com/EPFL-LCSB/etfl/-/tree/dev_yetfl. The supporting data is available in https://doi.org/10.5281/zenodo.4541577.

Acknowledgments

The authors would like to thank Dr. *Kaycie Butler* for her help in improving the wording and structure of this manuscript. This work has received funding from the European Union's Horizon 2020 research and innovation programme under grant agreement No 814408 (OO), the Swiss National Science Foundation under grant agreement 200021_188623 (OO), the European Union's Horizon 2020 Research and Innovation Programme under the Marie Skłodowska-Curie grant agreement No. 722287 (PS), the European Union's Horizon 2020 research and innovation program under the Marie Skłodowska Curie grant agreement No 675585 (MM), and the École Polytechnique Fédérale de Lausanne.

Author contribution

OO, PS and VH designed the study. OO and PS wrote the code to adapt ETFL to eukaryotic organisms. OO ran the simulations and did the enzymatic data curation. OO, LM and VH analyzed the results and provided the discussion. MC, MM and LM performed the thermodynamic curation of the Yeast8 GEM. OO, PS, MM, LM and VH wrote and reviewed the manuscript.

Table 1: Properties of the yETFL (variable biomass composition with thermodynamics) model created from Yeast8.3.4.

	yETFL
Growth upper bound (ū)	0.75 h^{-1}
Number of bins (N)	128
Resolution (ū/N)	0.0058 h^{-1}
Number of species	
- Metabolites	2689
- mRNAs	1393
- Peptides	1393
- rRNAs	6
Number of enzymes	
- Metabolic enzymes	1059
- RNA polymerases	2
- Ribosomes	3
Number of reactions	
- Metabolic	2678
- Transport	1047
- Exchange flux	243
- Transcription	1393
- Translation	1393
- Complexation	1065
- Degradation	2458
Thermodynamic data	
- Number of metabolites $\Delta G'^{\circ}_{f}$	2433
- Number of reactions $\Delta G'^{\circ}_{r}$	3184
- Percent of metabolites $\Delta G'^{\circ}_{f}$	90%
- Percent of reactions $\Delta G'^{\circ}_{r}$	80%

544 *Table 2:* The nomenclature, number of variables, and constraints of different ETFL models. EFL denotes Expression
545 and Flux. T denotes Thermodynamic. .cb and .vb represent constant and variable biomass composition, respectively.

Abbreviated name	Thermodynamics	Growth-dependent biomass composition	Number of variables	Number of constraints
EFL.cb	No	No	43,527	70,918
ETFL.cb	Yes	No	66,714	92,338
EFL.vb	No	Yes	43,565	71,012
ETFL.vb	Yes	Yes	66,746	92,429

546

Table 3: Gene essentiality results for (A) only metabolic genes (FBA and E[T]FL.cb) and (B) metabolic and expression genes (E[T]FL.cb) compared with experimental results. Matthew's correlation coefficient (MCC) was used as a metric to assess the quality of the predictions.

(A)	FBA, E[T]FL.cb (metabolic genes) MCC = 0.48	Predictions	
		Essential	Non-essential
Experimental	Essential	53	106
	Non-essential	12	945

(B)	E[T]FL.cb (metabolic and expression genes) MCC = 0.50	Predictions	
		Essential	Non-essential
Experimental	Essential	72	118
	Non-essential	16	1132

551

552

(A)

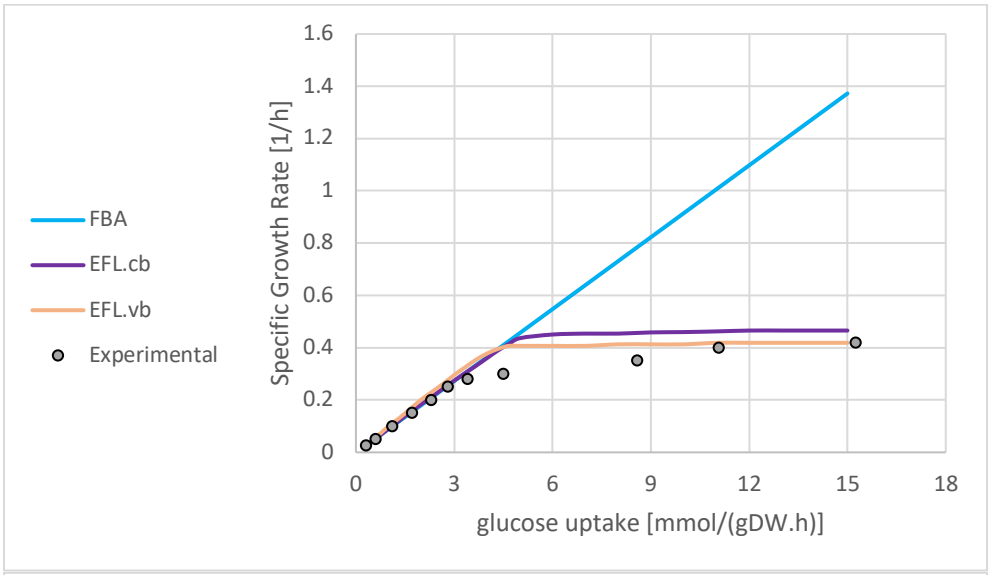

(B)

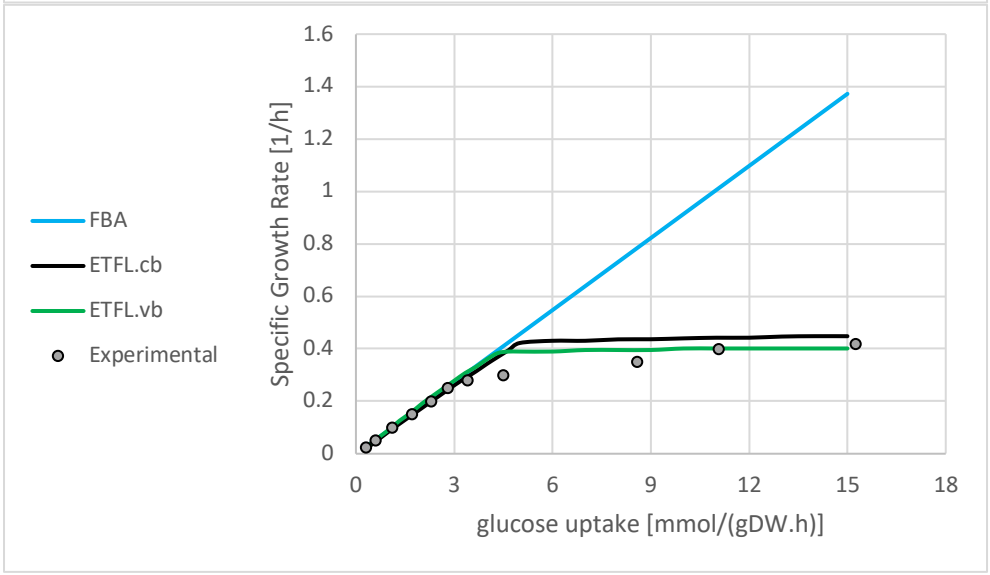

553

554

555 *Figure 1:* The maximum specific growth rate (h^{-1}) at different glucose uptake rates (mmol/(gDW.h)) for models (A)
556 with and (B) without thermodynamic constraints. The results are shown for the FBA model and ETFL models with
557 constant (E[T]FL.cb) and variable (E[T]FL.vb) biomass composition. The experimental data were taken from van
558 Hoek *et al.*[24].

(A)

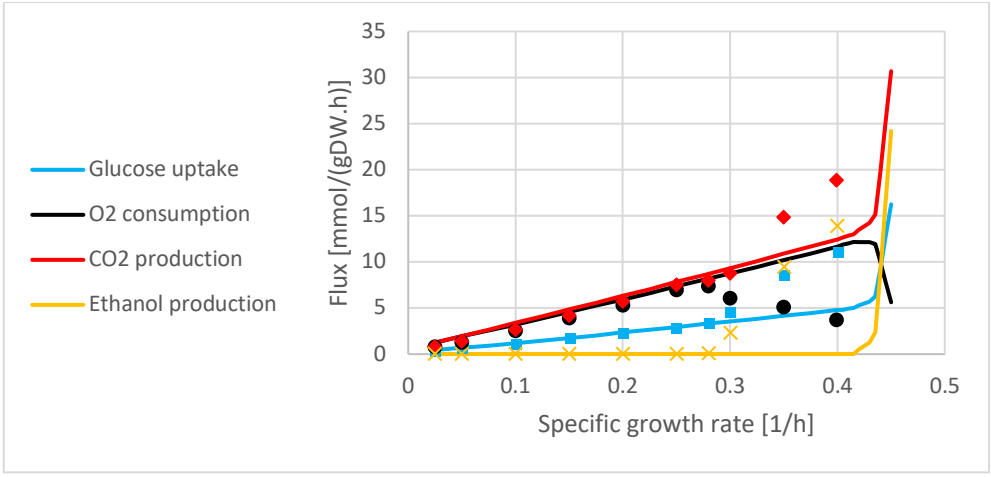

(B)

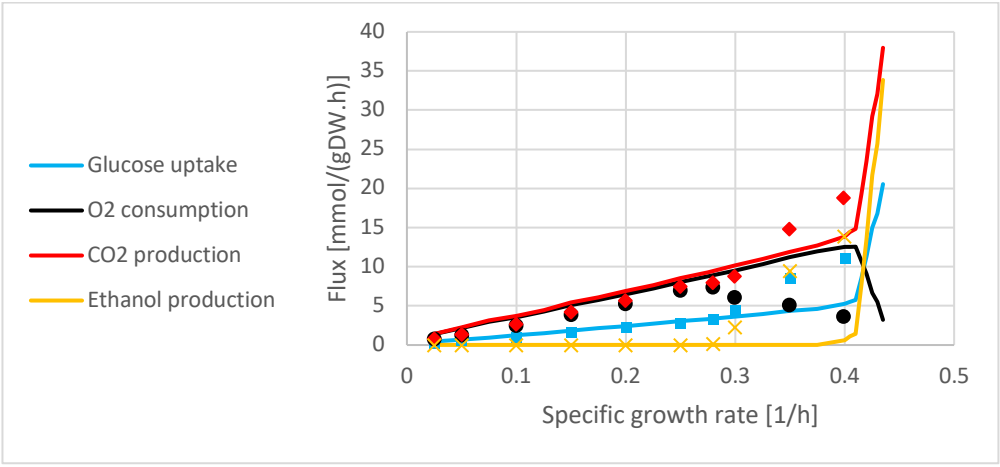

(C)

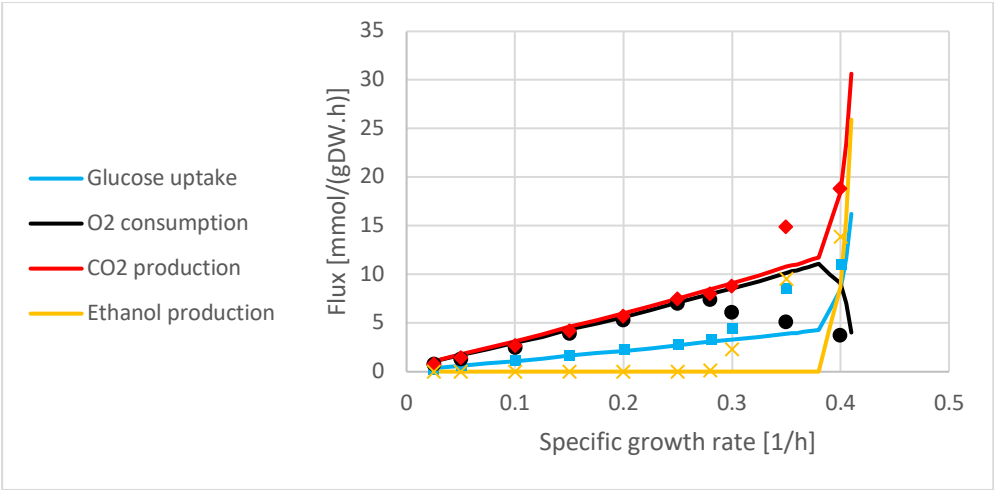

(D)

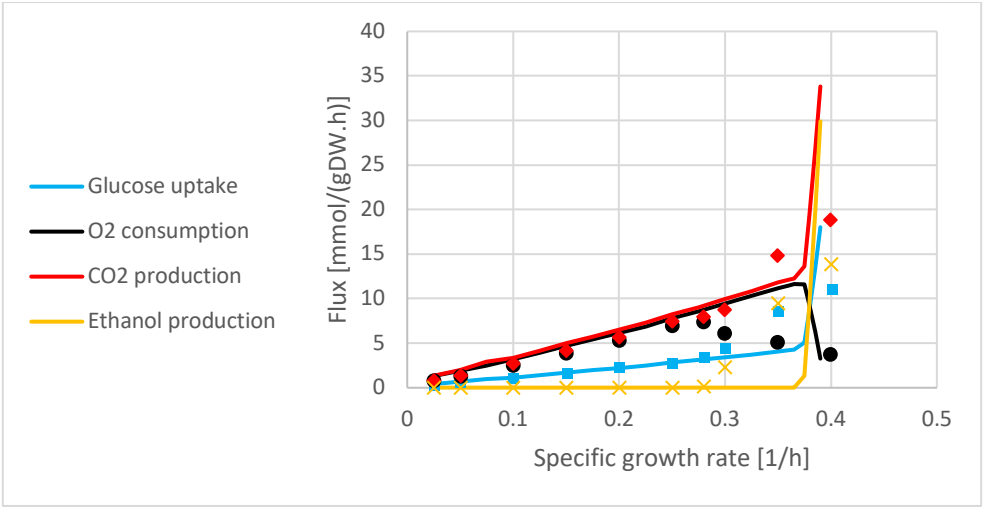

Figure 2: The simulation of the Crabtree effect for (A) EFL.cb, (B) ETFL.cb, (C) EFL.vb, and (D) ETFL.vb models. The experimental data were taken from van Hoek *et al.*[24].

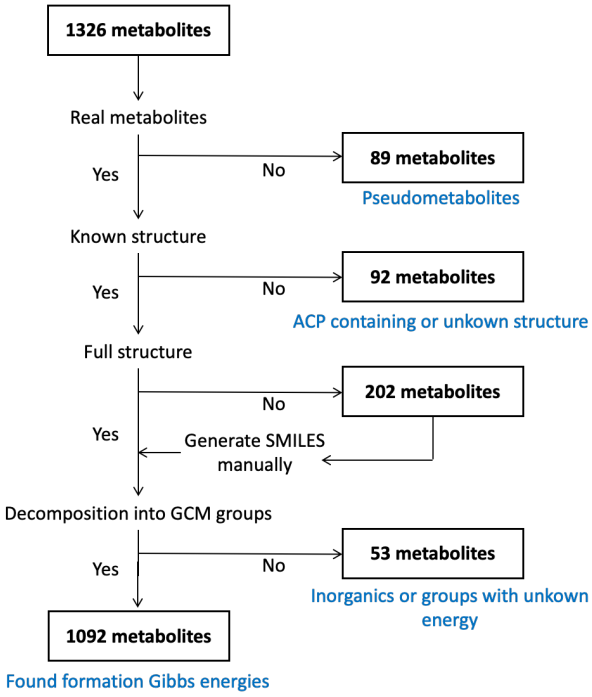

Figure 3: Schematic representation of the thermodynamic curation of the metabolites in Yeast8. Abbreviations: ACP: Acyl Carrier Protein; GCM: Group Contribution Method; SMILES: Simplified Molecular Input Line Entry System.

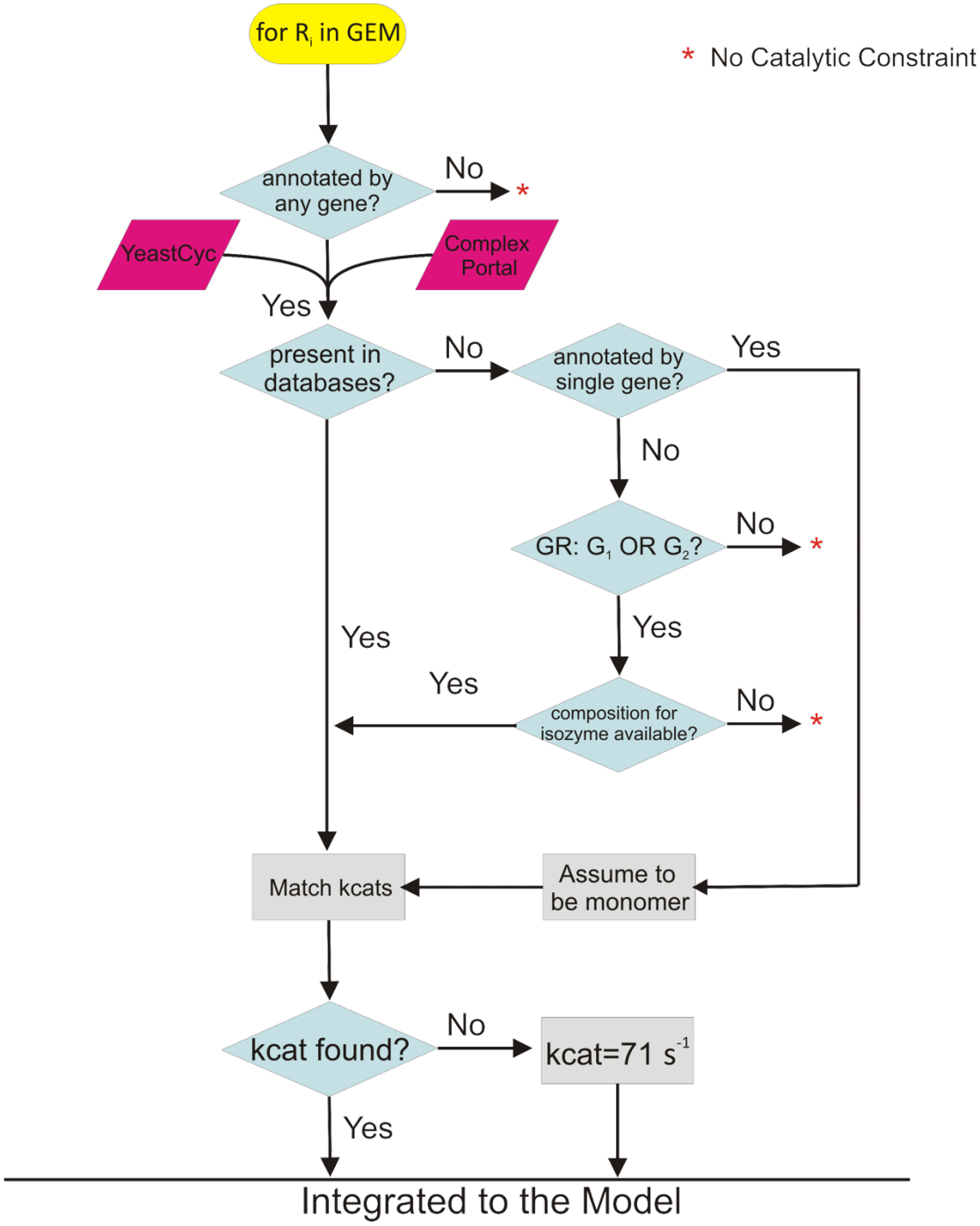

Figure 4: Workflow for the integration of enzymes into the model. The enzyme composition for the complex enzymes was sourced from YeastCyc and ComplexPortal. We used the function Match Kcats from GECKO[10] to find turnover numbers.

References

1. Borodina, I. & Nielsen, J. Advances in metabolic engineering of yeast Saccharomyces cerevisiae for production of chemicals. *Biotechnology journal* **9**, 609-620 (2014).
2. Gonçalves, F., Colen, G. & Takahashi, J. Yarrowia lipolytica and its multiple applications in the biotechnological industry. *The Scientific World Journal* **2014** (2014).
3. Kim, J.Y., Kim, Y.-G. & Lee, G.M. CHO cells in biotechnology for production of recombinant proteins: current state and further potential. *Applied microbiology and biotechnology* **93**, 917-930 (2012).
4. Gu, C., Kim, G.B., Kim, W.J., Kim, H.U. & Lee, S.Y. Current status and applications of genome-scale metabolic models. *Genome biology* **20**, 121 (2019).
5. Chiappino-Pepe, A., Pandey, V., Ataman, M. & Hatzimanikatis, V. Integration of metabolic, regulatory and signaling networks towards analysis of perturbation and dynamic responses. *Current Opinion in Systems Biology* **2**, 59-66 (2017).
6. Orth, J.D., Thiele, I. & Palsson, B.Ø. What is flux balance analysis? *Nature biotechnology* **28**, 245-248 (2010).
7. Schellenberger, J. et al. Quantitative prediction of cellular metabolism with constraint-based models: the COBRA Toolbox v2. 0. *Nature protocols* **6**, 1290 (2011).
8. Henry, C.S., Broadbelt, L.J. & Hatzimanikatis, V. Thermodynamics-based metabolic flux analysis. *Biophysical journal* **92**, 1792-1805 (2007).
9. Soh, K.C. & Hatzimanikatis, V. in Metabolic Flux Analysis 49-63 (Springer, 2014).
10. Sánchez, B.J. et al. Improving the phenotype predictions of a yeast genome-scale metabolic model by incorporating enzymatic constraints. *Molecular systems biology* **13**, 935 (2017).
11. Lerman, J.A. et al. In silico method for modelling metabolism and gene product expression at genome scale. *Nature communications* **3**, 929 (2012).
12. O'brien, E.J., Lerman, J.A., Chang, R.L., Hyduke, D.R. & Palsson, B.Ø. Genome-scale models of metabolism and gene expression extend and refine growth phenotype prediction. *Molecular systems biology* **9** (2013).
13. Salvy, P. & Hatzimanikatis, V. The ETFL formulation allows multi-omics integration in thermodynamics-compliant metabolism and expression models. *Nat Commun* **11**, 1-17 (2020).
14. Lloyd, C.J. et al. COBRAme: A computational framework for genome-scale models of metabolism and gene expression. *Plos Comput Biol* **14**, e1006302 (2018).
15. Krivoruchko, A. & Nielsen, J. Production of natural products through metabolic engineering of Saccharomyces cerevisiae. *Current opinion in biotechnology* **35**, 7-15 (2015).
16. Satyanarayana, T. & Kunze, G. Yeast diversity in human welfare. (Springer, 2017).

17. Förster, J., Famili, I., Fu, P., Palsson, B.Ø. & Nielsen, J. Genome-scale reconstruction of the Saccharomyces cerevisiae metabolic network. *Genome research* **13**, 244-253 (2003).
18. Heavner, B.D., Smallbone, K., Barker, B., Mendes, P. & Walker, L.P. Yeast 5–an expanded reconstruction of the Saccharomyces cerevisiae metabolic network. *BMC systems biology* **6**, 55 (2012).
19. Heavner, B.D., Smallbone, K., Price, N.D. & Walker, L.P. Version 6 of the consensus yeast metabolic network refines biochemical coverage and improves model performance. *Database* **2013** (2013).
20. Aung, H.W., Henry, S.A. & Walker, L.P. Revising the representation of fatty acid, glycerolipid, and glycerophospholipid metabolism in the consensus model of yeast metabolism. *Industrial biotechnology* **9**, 215-228 (2013).
21. Chowdhury, R., Chowdhury, A. & Maranas, C.D. Using gene essentiality and synthetic lethality information to correct yeast and CHO cell genome-scale models. *Metabolites* **5**, 536-570 (2015).
22. Lu, H. et al. A consensus S. cerevisiae metabolic model Yeast8 and its ecosystem for comprehensively probing cellular metabolism. *Nature communications* **10**, 1-13 (2019).
23. Monod, J. The growth of bacterial cultures. *Annual review of microbiology* **3**, 371-394 (1949).
24. Van Hoek, P., Van Dijken, J.P. & Pronk, J.T. Effect of specific growth rate on fermentative capacity of baker's yeast. *Appl. Environ. Microbiol.* **64**, 4226-4233 (1998).
25. van Hoek, P., van Dijken, J.P. & Pronk, J.T. Regulation of fermentative capacity and levels of glycolytic enzymes in chemostat cultures of Saccharomyces cerevisiae. *Enzyme and microbial technology* **26**, 724-736 (2000).
26. Boender, L.G., de Hulster, E.A., van Maris, A.J., Daran-Lapujade, P.A. & Pronk, J.T. Quantitative physiology of Saccharomyces cerevisiae at near-zero specific growth rates. *Appl. Environ. Microbiol.* **75**, 5607-5614 (2009).
27. Kasemets, K., Nisamedtinov, I., Laht, T.-M., Abner, K. & Paalme, T. Growth characteristics of Saccharomyces cerevisiae S288C in changing environmental conditions: auxo-accelerostat study. *Antonie Van Leeuwenhoek* **92**, 109-128 (2007).
28. Neidhardt, F.C. Escherichia coli and Salmonella. *Typhimurium Cellular and Molecular Biology* (1987).
29. Karpinets, T.V., Greenwood, D.J., Sams, C.E. & Ammons, J.T. RNA: protein ratio of the unicellular organism as a characteristic of phosphorous and nitrogen stoichiometry and of the cellular requirement of ribosomes for protein synthesis. *BMC biology* **4**, 30 (2006).
30. Vander Heiden, M.G., Cantley, L.C. & Thompson, C.B. Understanding the Warburg effect: the metabolic requirements of cell proliferation. *science* **324**, 1029-1033 (2009).
31. Xu, B., Jahic, M. & Enfors, S.O. Modeling of Overflow Metabolism in Batch and Fed-Batch Cultures of Escherichiacoli. *Biotechnology progress* **15**, 81-90 (1999).

32. Beg, Q.K. et al. Intracellular crowding defines the mode and sequence of substrate uptake by Escherichia coli and constrains its metabolic activity. *Proceedings of the National Academy of Sciences* **104**, 12663-12668 (2007).
33. Kremling, A., Geiselmann, J., Ropers, D. & de Jong, H. Understanding carbon catabolite repression in Escherichia coli using quantitative models. *Trends in microbiology* **23**, 99-109 (2015).
34. Chen, Y. & Nielsen, J. Energy metabolism controls phenotypes by protein efficiency and allocation. *Proceedings of the National Academy of Sciences* **116**, 17592-17597 (2019).
35. Salvy, P. & Hatzimanikatis, V. Emergence of diauxie as an optimal growth strategy under resource allocation constraints in cellular metabolism. *bioRxiv* (2020).
36. Macklin, D.N., Ruggero, N.A. & Covert, M.W. The future of whole-cell modeling. *Current opinion in biotechnology* **28**, 111-115 (2014).
37. Mavrovouniotis, M.L. Group contributions for estimating standard Gibbs energies of formation of biochemical compounds in aqueous solution. *Biotechnology and bioengineering* **36**, 1070-1082 (1990).
38. Alberty, R.A. Calculation of standard transformed Gibbs energies and standard transformed enthalpies of biochemical reactants. *Archives of biochemistry and biophysics* **353**, 116-130 (1998).
39. Kanehisa, M. & Goto, S. KEGG: kyoto encyclopedia of genes and genomes. *Nucleic acids research* **28**, 27-30 (2000).
40. Caspi, R. et al. The MetaCyc Database of metabolic pathways and enzymes and the BioCyc collection of Pathway/Genome Databases. *Nucleic acids research* **36**, D623-D631 (2007).
41. Meldal, B.H. et al. The complex portal-an encyclopaedia of macromolecular complexes. *Nucleic acids research* **43**, D479-D484 (2014).
42. Yuan, Q. et al. Pathway-consensus approach to metabolic network reconstruction for Pseudomonas putida KT2440 by systematic comparison of Published Models. *PloS one* **12** (2017).
43. Chan, S.H., Cai, J., Wang, L., Simons-Senftle, M.N. & Maranas, C.D. Standardizing biomass reactions and ensuring complete mass balance in genome-scale metabolic models. *Bioinformatics* **33**, 3603-3609 (2017).
44. Lange, H. & Heijnen, J. Statistical reconciliation of the elemental and molecular biomass composition of Saccharomyces cerevisiae. *Biotechnology and bioengineering* **75**, 334-344 (2001).
45. Gombert, A.K., dos Santos, M.M., Christensen, B. & Nielsen, J. Network identification and flux quantification in the central metabolism of Saccharomyces cerevisiae under different conditions of glucose repression. *Journal of bacteriology* **183**, 1441-1451 (2001).
46. Wang, M. et al. PaxDb, a database of protein abundance averages across all three domains of life. *Molecular & cellular proteomics* **11**, 492-500 (2012).
47. Alberts, B. Molecular Biology of the Cell: Hauptbd. (Garland, 2002).
48. Planta, R.J. & Mager, W.H. The list of cytoplasmic ribosomal proteins of Saccharomyces cerevisiae. *Yeast* **14**, 471-477 (1998).

49. GRAACK, H.-R. & Wittmann-Liebold, B. Mitochondrial ribosomal proteins (MRPs) of yeast. *Biochemical Journal* **329**, 433-448 (1998).
50. Thiele, I. & Palsson, B.Ø. A protocol for generating a high-quality genome-scale metabolic reconstruction. *Nature protocols* **5**, 93 (2010).
51. Joyce, A.R. & Palsson, B.Ø. in Microbial Gene Essentiality: Protocols and Bioinformatics 433-457 (Springer, 2008).
52. Lewis, N.E. et al. Omic data from evolved E. coli are consistent with computed optimal growth from genome-scale models. *Molecular systems biology* **6** (2010).
53. Salvy, P. et al. pyTFA and matTFA: a Python package and a Matlab toolbox for Thermodynamics-based Flux Analysis. *Bioinformatics* **35**, 167-169 (2019).
54. Ebrahim, A., Lerman, J.A., Palsson, B.O. & Hyduke, D.R. COBRApy: COnstraints-based reconstruction and analysis for python. *BMC systems biology* **7**, 74 (2013).
55. Jensen, K., Cardoso, J. & Sonnenschein, N. Optlang: An algebraic modeling language for mathematical optimization. *The Journal of Open Source Software* (2016).